Slow Relaxation Dynamics of Tubular Polymersomes after Thermal Quench

2 AUTHORS:

Antje Reinecke
Max Planck Institute of Colloids and Interfaces
8 PUBLICATIONS   **336** CITATIONS

SEE PROFILE

Hans-Günther Döbereiner
Universität Bremen
55 PUBLICATIONS   **3,007** CITATIONS

SEE PROFILE

Slow Relaxation Dynamics of Tubular Polymersomes after Thermal Quench

Antje A. Reinecke and Hans-Günther Döbereiner*

Max-Planck-Institut of Colloids and Interfaces, Am Mühlenberg 1, 14476 Golm, Germany

Morphological shape changes of giant tubular vesicles prepared from the diblock copolymer polybutadiene-(32)-*b*-polyethylene oxide(20) (PB−PEO) in aqueous solution after thermal quenches between 10 and 50 K were monitored via quantitative phase-contrast microscopy. Reducing the temperature leads to extremely slow sequential beading of the tubes where the formation of necks starts symmetrically at the two ends. We characterize the neck diameters and find that the necks close one by one with effective velocities on the order of a few tens of nanometers per minute. The necks do not close continuously, but rather their radii decrease in time in a sequence of exponential decays between intermediate plateaus. The slow dynamics is a result of the high membrane surface viscosity of PB−PEO. Sequential beading is rationalized via a cascade of metastable shapes determined by the bending elastic energy of the tubular polymersomes.

1. Introduction

Amphiphilic diblock copolymers self-assemble in selective solvents into supramolecular aggregates.[1−3] Depending on the polymeric architecture and solution conditions, a vast array of different structures are found.[4] In particular, multiple vesicular morphologies[5] including giant polymersomes[2,3] have been identified. Polymersomes are potentially interesting as mechanically[6,7] and rheologically[8] robust supramolecular containers. One can envision their possible usage for drug delivery, gene therapy, and waste removal and as chemical microreactors. Cross-linked polymersome membranes[9] exhibit a remarkable toughness with broadly adjustable properties. To understand material behavior, it is necessary in general to characterize the supramolecular architecture and probe its response to changes in a variety of solution parameters such as solvent content, salinity, or temperature. Direct visualization of polymeric aggregates by cryogenic transmission electron microscopy provides information on structural details[10] and the kinetics of transitions between different aggregate morphologies[11] on nanometer length scales. However, the resolution in time is somewhat limited by sample preparation. In the micrometer regime, it is possible to continuously record the dynamics of morphological transformations using phase-contrast

microscopy.[12−14] In this paper, we use this technique to monitor the morphological reaction of tubular polymersomes prepared from the diblock polybutadiene-*b*-polyethylene oxide[15] to fast temperature changes.

2. Elastic Energy Concept and Polymersome Shapes

The morphology of polymersomes is determined by the bending elastic energy[16−18] of their bilayer membrane.[2,8] Although a single giant polymersome is typically not in chemical equilibrium with the bulk, forces acting on the membrane balance, establishing local mechanical equilibrium. In analogy to lipid vesicles,[19−23] polymersomes assume the shape which corresponds to the minimal elastic energy at a given vesicle volume and area.[24] The vesicle volume is constant because of the osmotic balance across the membrane, which equilibrates the internal and external solute concentrations. The vesicle area is a function of temperature. Besides geometrical constraints, the parameter most important for determining the vesicle shape is the spontaneous curvature of its membrane.[25−27] Variations in this parameter, induced, e.g., via temperature changes, control the vesicle morphology and may lead to transitions between different shape classes. One of the most prominent examples is the budding transi-

* To whom correspondence should be addressed. E-mail: hgd@mpikg-golm.mpg.de.

(1) Zhang, L.; Eisenberg, A. *Science* **1995,** *268,* 1728.
(2) Discher, B. M.; Won, Y.-Y.; Ege, D. S.; Lee, J. C-M.; Bates, F. S.; Discher, D. E.; Hammer, D. A. *Science* **1999,** *284,* 1143.
(3) Discher, D. E., Eisenberg, A. *Science* **2002,** *297,* 967.
(4) Cameron, N. S.; Corbierre, M. K.; Eisenberg, A. *Can. J. Chem.* **1999,** *77,* 1311.
(5) Burke, S.; Shen, H..; Eisenberg, A. *Macromol. Symp.* **2001,** *175,* 273−283.
(6) Lee, J. C.-M.; Bermudez, H.; Discher, B. M.; Sheehan, M. A.; Won, Y.-Y.; Bates, F. S.; Discher, D. E. *Biotechnol. Bioeng.* **2001,** *73,* 135.
(7) Aranda-Espinoza, H.; Bermudez, H.; Bates, F. S.; Discher, D. E. *Phys. Rev. Lett.* **2001,** *87,* 208301.
(8) Dimova, R.; Seifert, U.; Pouligny, B.; Förster, S.; Döbereiner, H.-G.; *Eur. Phys. J. E* **2002,** *7,* 241.
(9) Discher, B. M.; Bermudez, H.; Hammer, D. A.; Discher, Dennis E.; Won, Y.-Y.; Bates, F. S. *J. Phys. Chem. B* **2002,** *106,* 2848.
(10) Won, Y.-Y.; Brannan, A. K.; Davis, H. T.; Bates, F. S. *J. Phys. Chem. B* **2002,** *106,* 3354.
(11) Chen, L.; Shen, H.; Eisenberg, A. *J. Phys. Chem. B* **1999,** *103,* 9488.

(12) Döbereiner, H.-G.; Evans, E.; Seifert, U.; Wortis, M. *Phys. Rev. Lett.* **1995,** *75,* 3360.
(13) Döbereiner, H.-G.; Seifert, U. *Europhys. Lett.* **1996,** *36,* 325.
(14) Bar-Ziv, R.; Moses, E.; Nelson, P. *Biophys. J.* **1998,** *75,* 294.
(15) Förster, S. and Krämer, E. *Macromolecules* **1999,** *32,* 2783.
(16) Helfrich, W. *Z. Naturforsch.* **1974,** *29,* 510.
(17) Evans, E. *Biophys. J.* **1974,** *14,* 923.
(18) Lipowsky, R. *Nature* **1992,** *349,* 475.
(19) Berndl, K.; Käs, J.; Lipowsky, R.; Sackmann, E.; Seifert, U. *Europhys. Lett.* **1990,** *13,* 659.
(20) Käs, J.; Sackmann, E. *Biophys. J.* **1991,** *60,* 825.
(21) Miao, L.; Seifert, U.; Wortis, M.; Döbereiner, H.-G. *Phys. Rev. E* **1994,** *49,* 5389.
(22) Seifert, U. *Adv. Phys.* **1997,** *46,* 13.
(23) Döbereiner, H.-G. *Curr. Opin. Colloid Interface Sci.* **2000,** *5,* 256−263.
(24) Haluska, C. K.; Goźdź, W. T.; Döbereiner, H.-G.; Förster, S.; Gompper, G. *Phys. Rev. Lett.* **2002,** *89,* 238302.
(25) Döbereiner, H.-G.; Evans, E.; Kraus, M.; Seifert, U.; Wortis, M. *Phys. Rev. E* **1997,** *55,* 4458.
(26) Döbereiner, H.-G.; Selchow, O.; Lipowsky, R. *Eur. Biophys. J.* **1999,** *28,* 174.
(27) Lee, J.; Petrov, P. G.; Döbereiner, H.-G. *Langmuir* **1999,** *15,* 8543.

tion,[21,25] where a small satellite is expelled from a parent prolate vesicle as spontaneous curvature is increased.

At a sufficiently large volume-to-area ratio, the budding transition is first-order and budding proceeds from a metastable prolate shape.[25] Typically, this leads to the following scenario: A change in spontaneous curvature, which transports the vesicle across the budding transition, does not lead immediately to budding. Rather, the vesicle remains in a metastable state attempting to cross the activation barrier. Variation in the barrier height leads to a distribution of mean escape times out of the metastable configuration. Thus, there is typically a variable delay time after changes in the spontaneous curvature before the vesicle buds.

3. Materials and Protocols

Polymer. For our study we employed giant vesicles made from the diblock polybutadiene-*b*-polyethylene oxide (PB−PEO, *s*-Bu[CH$_2$CH(C$_2$H$_3$)]$_{32}$[OCH$_2$CH$_2$]$_{20}$OH).[15] The polydispersity in molecular weight was found to be $M_w/M_n = 1.05$, where M_n and M_w are the number- and weight-averaged molecular masses, respectively. The ratio of 1,2- versus 1,4-butadiene is 9:1. The dry polymer melt was stored in the freezer at −20 °C. Stock solutions were made using chloroform.

Vesicle Preparation. Vesicles were prepared using an adapted standard swelling procedure.[28] Briefly, a few drops (about 30 μL) of the polymer solution (40 mg/mL in chloroform) was spread on a roughened Teflon disk and dried under vacuum overnight. The sample was prehydrated and swollen in 100 mM sucrose solution at a temperature of 38 °C for a few hours. The vesicles were harvested and incubated in 110 mM excess glucose solution to allow for modest deflation and enhancement of contrast.

Viscoelastic Properties. Vesicle membranes obtained with the above procedure were in the fluid state at room temperature, albeit with a large surface viscosity, $\eta_s = 1.5 \times 10^{-6}$ Ns/m.[8] The elastic properties are characterized by a bending modulus of $\kappa = 42 \pm 5\ k_B T$ and an area stretching modulus of $K = 0.47 \pm 0.02$ N/m.[8]

Phase-Contrast Microscopy. A temperature-controlled observation chamber was filled with the vesicle solution, tightly sealed, and inspected under a phase-contrast microscope (Zeiss 135, 40×, Ph 2). Due to the inside sucrose solution, the vesicles are slightly heavier than the outside glucose solution and sink to the bottom of the chamber. Tubular vesicles are oriented mainly along the glass substrate but show thermal fluctuation out of the focal plane of the microscope. Suitable vesicles were selected and observed over time.

Thermal Trajectories. Fast temperature changes could be accomplished by using two thermal water baths at different temperatures connected to the observation chamber by a flow switching device. After a temperature jump, the chamber temperature was reached with a fast initial exponential relaxation time of about 50 s. The final desired chamber temperature was then approached more slowly with a deviation of only 0.5 °C after 5 min.

Measurement of Lengths. Neck diameters were measured from video frames obtained at regular time intervals using Photoshop. The nominal membrane position was taken at the point of maximum gradient in a gray value profile across the vesicle membrane. The total error for distance determination within one video frame is about 100 nm. Time series of neck diameters were smoothed by averaging over five consecutive frames to remove small-scale thermal fluctuations. Tube lengths were obtained by adding axial segments along the tube to correct for slight bending.

4. Results and Discussion

Tubular vesicles of various lengths and diameters were subject to thermal quench from high to low temperatures. We observed regularly that reducing the temperature between 10 and 50 K induced beading of the tubes starting
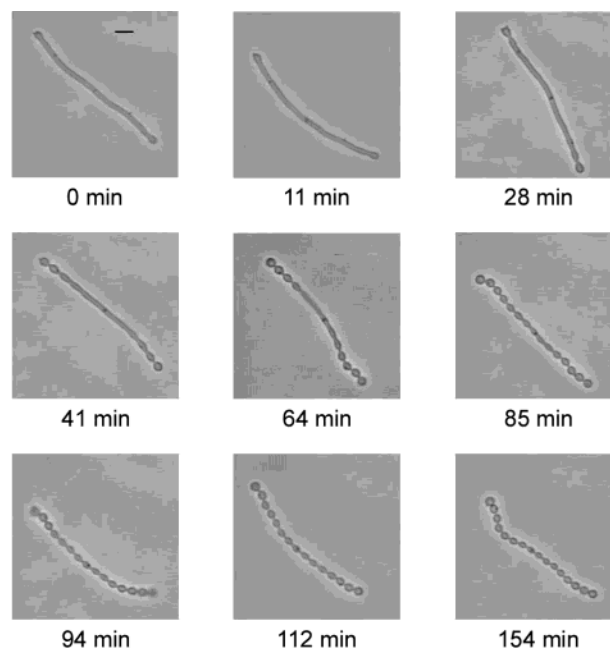
(28) Evans, E.; Needham, D. *J. Phys. Chem.* **1987**, *91*, 4219.

Figure 1. Sequential beading of a tubular polymersome. Shown are phase-contrast pictures of a tube in sucrose (inside)/glucose (outside) solution after a thermal quench from 38 to 25 °C. The initial diameter of the tube is 2.4 μm. The time elapsed after reducing the temperature is indicated below each picture: 0−28 min, there is a time delay before the vesicle starts to bead; 28 min, beginning of neck closure from the end of the tube; 28−94 min, progression of beading toward the tube center; 94−154 min, completely beaded tube. This configuration is stable in time. The bar corresponds to 10 μm.
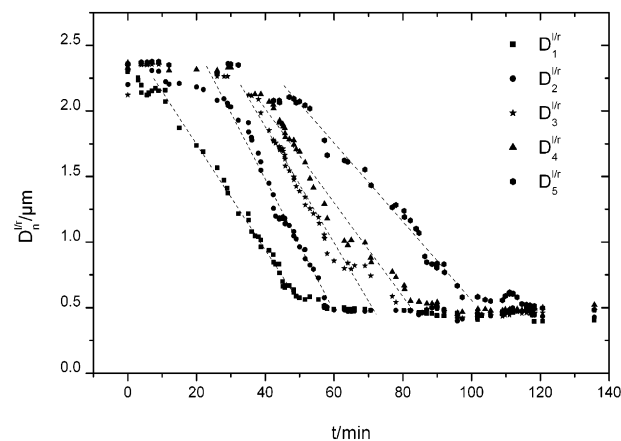

Figure 2. Sequential neck diameters as a function of time. The diameters of corresponding left (l) and right (r) necks are averaged and denoted by $D^{l/r}_n$. Plotted are numerical values obtained from the tube shown in Figure 1. One can identify nicely the closure of neck after neck. Note the quasi-linear time dependence. As a mean slope one finds 35 ± 5 nm/min. There is a typical, approximately constant time delay before subsequent neck diameters reach the same numerical value. It is found to be about 12 min for $D^{l/r}_n = 1$ μm in this example. The diameters of further necks are not shown for clarity. Due to shape fluctuations of the tube out of the focal plane, the neck diameters could not be measured continuously.

symmetrically from the two ends (see Figures 1 and 2 for a typical example). The gradual change of polymersome morphology proceeds at constant temperature and corresponds to the relaxation to a new equilibrium shape. However, the beading process was not seen in all cases. We also monitored vesicles which developed only slight undulations or did not react at all, even after large temperature changes. In several cases, we observed that
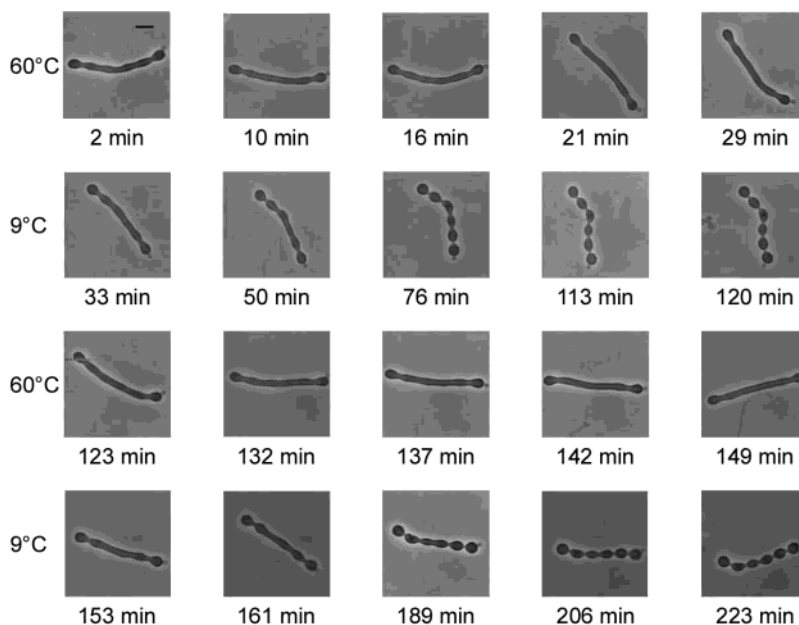
Figure 3. Thermal cycling of a polymersome. Shown are phase-contrast pictures of a tube in sucrose/glucose solution taken during thermal cycling at the time indicated below each picture. Between temperature changes at 30, 120, and 150 min, the sample is kept at the temperatures indicated. The vesicle exhibits reversible beading after each temperature quench. The bar corresponds to 10 μm.
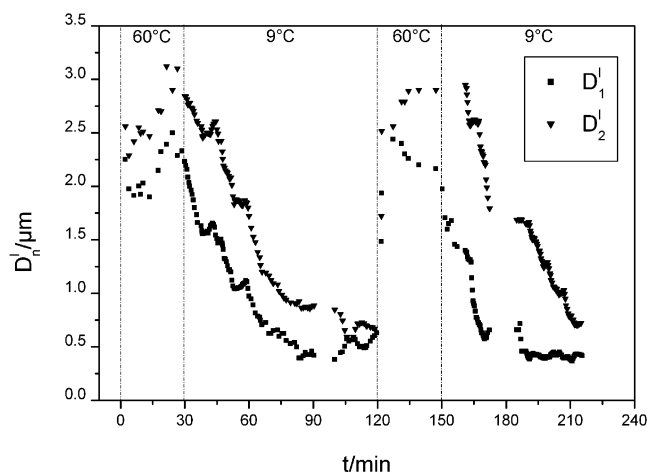

Figure 4. Thermal cycling of tube diameters D^l_n. The temperatures are indicated. Plotted are measurements of the first two, left neck diameters of the vesicle shown in Figure 3. There is a stepwise, reversible closing of the necks after each temperature quench.

Figure 5. Thermal area expansion of a tubular polymersome. The tube length L is plotted versus temperature T. The inset shows pictures of the tube corresponding to the (L, T) values given in the graph. The upper end of the vesicle for different temperatures is aligned along a horizontal line.

the tubes reacted only after a time delay which ranged from a few minutes to 1/2 h. Nevertheless, cycling the temperature on the *same* vesicle established reversibility and gave reproducible results (see Figures 3 and 4). In total, we monitored 21 vesicles in detail.

Variation of the temperature induces a corresponding change in the membrane area. In general, decreasing the temperature leads to shorter tubes (see Figure 5) and slightly larger radii (data not shown), consistent with a constant volume of the vesicle. Indeed, we find the scaling behavior $R^2 \sim L^{-1}$. Thus, we may obtain the thermal area expansion coefficient α_A from a linear plot of the normalized tube length L vs temperature T with slope $\alpha_L = L_0^{-1}$ dL/dT. In a very good approximation, we find $\alpha_A \approx 2\alpha_L = (2.8 \pm 0.6) \times 10^{-3}$/$K$ from a measurement of six tubes. This is consistent with results reported in ref 6 for a similar diblock copolymer.

The vesicle end-to-end distance reacts in a characteristic way to temperature reduction (see Figure 6). One observes
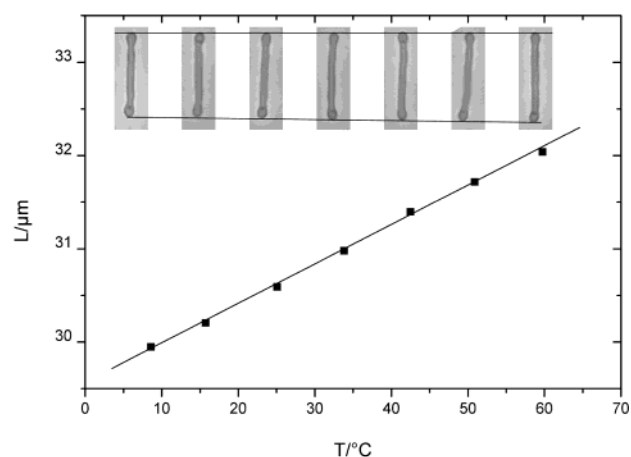
an instantaneous initial reduction of the tube length, reflecting a change in tube area with temperature. Some time after a temperature quench, which varies with the initial conditions of the vesicle, beading starts. This leads to a further reduction in the end-to-end distance of the polymersome, reflecting the morphological change from a tube to a string of beads. Tube beading is reversible and can be cycled several times as shown.

We can very well rationalize these observations by noting that (a) tubular vesicles belong to the prolate class in the phase diagram of vesicle shapes,[21,23] (b) beading corresponds to budding transitions into multiply budded configurations, and (c) reducing the temperature induces an increase of the membrane spontaneous curvature in our system as found already in thermal trajectories of high genus vesicles.[24] The phase diagram of vesicle shapes depends on the volume-to-area ratio v and spontaneous curvature c_0. At fixed v, there is a sequence of shape classes from more inwardly to more outwardly curved vesicles as c_0 increases. Especially, prolate (large v) or tubular (small
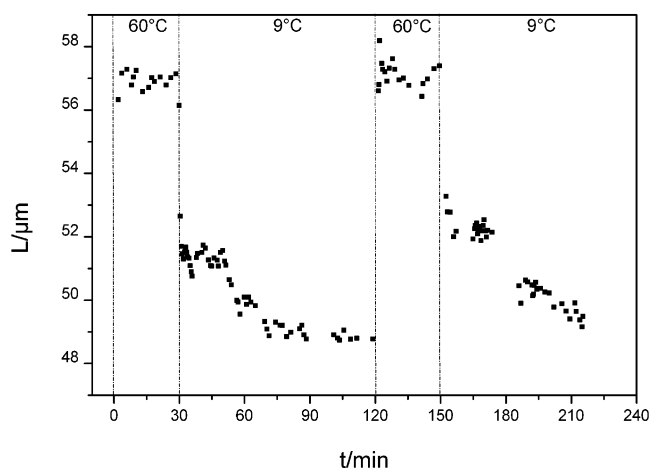
Figure 6. Thermal cycling of the tube length *L*. The temperatures are indicated. Plotted are measurements taken from the vesicle shown in Figure 3.

v) vesicles become unstable to budded shapes at some particular value of spontaneous curvature. Depending on the initial conditions of a particular tubular vesicle, it is located at different points in the phase diagram. Therefore, increasing the spontaneous curvature by a constant amount via reducing the temperature results in a more or less deep quench into a budded phase and, correspondingly, in different levels of beading. In addition, one expects metastable tubular shapes with varying relaxation times into a stable budded configuration, as discussed in section 2.

The beading process always starts at the end of the vesicles moving further along the tube as time progresses (see Figure 2), establishing a beading front. This is likely due to the fact that there is always a slight neck visible at the two ends of the tubular vesicles. This is true even when the rest of the vesicle appears as a straight tube with a constant diameter along the long axis of the vesicle body (see Figure 5). Thus, decreasing the radius of the first neck is energetically most favorable for initiating the sequential budding process induced by the increase in spontaneous curvature. Closing of further necks then happens in a slow cascade-like process. As is evident from time series of neck diameters (see Figure 4), there are intermediate metastable states with an increasing degree of neck closure as the vesicle diffuses along the most favorable path in the bending energy landscape. The vesicle shape gets temporarily caught in these metastable states. Characteristic mean escape times out of one of these states and characteristic relaxation times into the next one, both on the order of 10 min, lead to a cascade of exponential relaxation processes between subsequent plateaus with progressively smaller neck diameters. On a coarse-grained time scale, the cascade appears as a quasi-linear reduction in neck diameter, as seen in Figure 2 for subsequent necks. One finds typical velocities of a few tens of nanometers per minute for neck closure and front propagation. The slow dynamics of this process is due to the large surface viscosity η_s of PB−PEO, which leads to dissipation in the membrane rather than in bulk water.[8] The natural velocity scale is given by $v = \kappa/\eta_s D$. Inserting a typical value for the tube diameter, $D = 2\ \mu$m, and using the surface viscosity and bending modulus of PB−PEO, we find $v = 100$ nm/s, which is about two orders of magnitude faster than the velocities measured in experiment. Opening of the necks at high temperature is considerably quicker than closing at low temperature.

Besides possible different elastic driving forces for neck closure and opening, a likely explanation for this behavior is that the membrane viscosity is indeed lower at elevated temperatures.

A similar morphological transition of long tubular membranes, where a string of pearls forms, can be induced by pulling on them with laser tweezers.[14,29−32] The so-called pearling instability, observed with lipid membranes, is analogous to the well-known Rayleigh instability of a fluid cylinder breaking up into spherical droplets. However, our measurements and the laser tweezers experiments[14,29,32] are performed in different ensembles and with different types of amphiphiles. Whereas the volume and area of our tubular polymersomes are conserved during a temperature quench, the application of axial force via laser tweezers effectively controls membrane tension. Even though the two ensembles are related by a Legendre transformation, the stability regions of the shapes[33] are different in each ensemble.[22] Thus, we cannot establish a direct correspondence. In fact, as discussed above, the appropriate parameters in our case are the volume-to-area ratio of the vesicle and the effective spontaneous curvature of its membrane.[21] Moreover, the dynamics of lipid membranes is governed by dissipation in water, whereas polymersomes dissipate elastic bending energy within their membrane. Nevertheless, we note that front propagation is found in pearling as well and proceeds considerably slower than the characteristic velocity for the lipid tubules, $v = \kappa/\eta D^2$, where η is the viscosity of water.[31,32] Indeed, that is what we observe in our system. Interestingly, there is also a delay time after application of tension before pearling starts in lipid tubules.[32] For our polymersomes, we argued above that the observed delay after temperature quench corresponds to the mean escape time out of a metastable tubular state.

In this paper, we monitored morphological changes of polymersomes induced by temperature quenches using quantitative phase-contrast microscopy. The membrane dynamics was found to be extremely slow. It seems feasible to extend these studies to sudden variations in general environmental conditions by transferring vesicles into different solutions via micropipet manipulation.[34] Compared to lipids, synthetic polymer chains offer an ample diversity in designing novel artificial membranes with tailor-made mechanical characteristics. The possibility to include polymeric segments that respond specifically to pH, ionic strength, or temperature allows membrane functions to be controlled in different biological environments.

(29) Bar-Ziv, R.; Moses, E. *Phys. Rev. Lett.* **1994**, *73*, 1392.
(30) Nelson, P.; Powers, T.; Seifert, U. *Phys. Rev. Lett.* **1995**, *74*, 3384.
(31) Goldstein, R. E.; Nelson, P.; Powers, T.; Seifert, U. *J. Phys. II* **1996**, *6*, 767.
(32) Bar-Ziv, R.; Tlusty, T.; Moses, E. *Phys. Rev. Lett.* **1997**, *79*, 1158.
(33) Bukman, D. J.; Yao, J. H.; Wortis, M. *Phys. Rev. E* **1996**, *54*, 5463.
(34) Xu, L.; Döbereiner, H.-G. *Perspect. Supramol. Chem.* **2000**, *6*, 181−184.